REVIEW ARTICLE
https://doi.org/10.1038/s41929-018-0138-x

nature catalysis

Catalytic conversion of solar to chemical energy on plasmonic metal nanostructures

Umar Aslam, Vishal Govind Rao, Steven Chavez and Suljo Linic*

The demonstrations of visible-light-driven chemical transformations on plasmonic metal nanostructures have led to the emergence of a new field in heterogeneous catalysis known as plasmonic catalysis. The excitement surrounding plasmonic catalysis stems from the ability to use the excitation of energetic charge carriers (as opposed to heat) to drive surface chemistry. This offers the opportunity to potentially discover new, more selective reaction pathways that cannot be accessed in temperature-driven catalysis. In this Review, we provide a fundamental overview of plasmonic catalysis with emphasis on recent advancements in the field. It is our objective to stress the importance of the underlying physical mechanisms at play in plasmonic catalysis and discuss possibilities and limitations in the field guided by these physical insights.

Metal nanoparticles are an important class of materials used as heterogeneous catalysts for a number of industrial chemical transformations including dehydrogenations, partial oxidations, reduction reactions, ammonia synthesis and hydrocarbon reforming, among others[1–13]. These processes are typically performed at relatively high temperatures to provide sufficient energy for activating chemical bonds on the surfaces of the nanoparticles[14,15]. An unavoidable side effect of this approach is that energy is deposited into every available reaction coordinate. This can result in the simultaneous activation of unselective reaction pathways leading to the undesirable formation of by-products and chemical waste. An alternative mechanism for activating chemical bonds on metal surfaces involves the excitation of energetic charge carriers (typically via photoexcitation) into the reactants (adsorbates)[16–20]. These electronic excitations can lead to chemical transformation. Under this mechanism, it is in principle possible to have improved control over the outcome of chemical reactions by specifically targeting electronic excitations that result in the preferential activation of desired chemical transformations.

Early observations of charge-carrier-mediated reactions on metals were primarily made on extended metal surfaces in the 1980s and 1990s[21–24]. In these studies, high-intensity lasers were used to excite energetic charge carriers at appreciable rates near the adsorbate/metal interface. The need to use high-intensity lasers to achieve measurable rates made this mechanism of activating chemical reactions generally impractical for technological applications such as heterogeneous catalysis. In recent years, however, it has been shown that plasmonic metal nanoparticles can perform charge-carrier-mediated reactions under lower-intensity visible light illumination, of the order of solar intensity[25–27]. These findings have reignited interest in charge-carrier-mediated chemical transformations on metal surfaces and led to the emergence of a vibrant, new area of research in heterogeneous catalysis known as plasmonic catalysis[28–31].

In this Review, we will provide an overview of plasmonic catalysis with emphasis on recent advancements, discuss the limitations of plasmonic catalysis, and comment on future directions in the field. We begin by introducing plasmonic metal nanoparticles and their interaction with light through the excitation of localized surface plasmon resonance. This is followed by a discussion of the mechanisms of energy transfer from plasmonic metals to reactants and the resulting charge carrier-mediated activation of chemical bonds. We then describe the limitations of plasmonic catalysis on monometallic nanostructures and possibilities for guiding plasmonic energy to more reactive, non-plasmonic sites. Finally, we conclude by providing our perspective on the current state of the field and opportunities for further advancements.

Plasmonic metal nanoparticles

Plasmonic metal nanoparticles are light-harvesting materials that interact with visible light through the excitation of localized surface plasmon resonance (LSPR)[32,33]. LSPR is established when light of wavelengths longer than the size of the metal nanoparticles causes a resonant, collective oscillation of the free electrons in the metal nanoparticles. This physical process allows the nanoparticles to collect the energy of visible light, concentrate it near the surface of the particles, and ultimately convert light energy into the energy of excited charge carriers. We present a detailed discussion of these processes in the following sections.

Optical properties of plasmonic nanoparticles. A key characteristic of plasmon excitation is a large optical extinction cross-section of the metal nanoparticles at resonant frequencies due to a collective excitation of electrons[34,35]. At the LSPR frequencies, the extinction cross-section of plasmonic nanoparticles can be up to ten times their geometric cross-section for single nanoparticles and even larger for nanoparticle clusters[36]. For a spherical nanoparticle, using Mie approximation, the extinction cross section (σ_{ext}) is related to the complex dielectric function of the metal as follows:

$$\sigma_{ext} \sim \frac{\varepsilon_2}{[\varepsilon_1 + 2\varepsilon_m]^2 + \varepsilon_2^2} \quad (1)$$

where ε_1 is the real part of the dielectric function of the metal, ε_2 is the imaginary part of the dielectric function of the metal and ε_m is the dielectric constant of the medium[37,38]. This relationship helps us identify physical criteria that must be satisfied for a metal to undergo plasmon excitation. It is clear that the extinction cross-section is the largest as the denominator approaches zero. This stipulates that $\varepsilon_1 \approx -2\varepsilon_m$ and ε_2 should be small for plasmon excitation to occur.

Department of Chemical Engineering, University of Michigan, Ann Arbor, MI, USA. *e-mail: linic@umich.edu

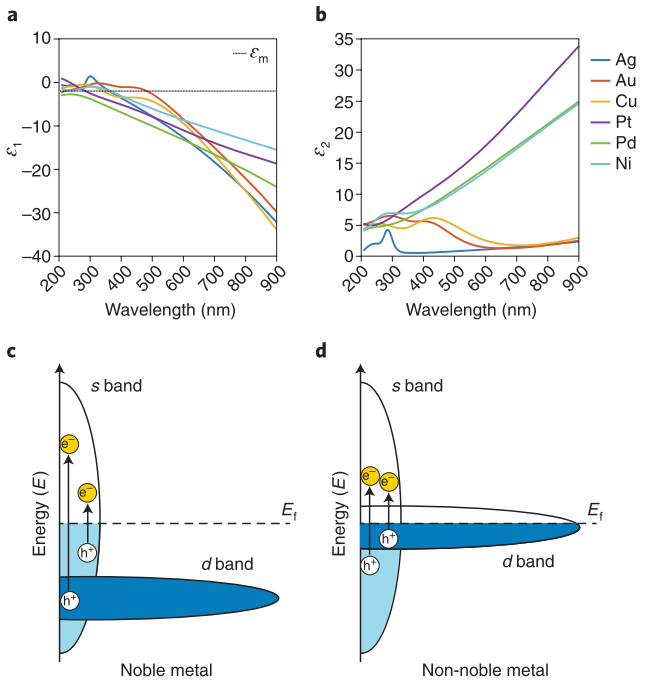

Fig. 1 | Dielectric properties of metals. a, The real part of the dielectric function for the plasmonic metals (Ag, Cu, Au) and other transition metals. The black line represents the case where $\varepsilon_1 = -2\varepsilon_{m,air}$. **b**, The imaginary part of the dielectric function for the plasmonic metals and other transition metals. **c**,**d**, Sketches of the representative density of states of a plasmonic metal (**c**) and non-noble transition metal (**d**). Intraband *s*-to-*s* transitions are accessible with visible light photons for all metals. As the *d* band lies far before the Fermi level (E_f) for plasmonic metals, only high-energy photons can induce interband *d*-to-*s* excitations for these metals. In the case of non-noble metals, the *d* band intersects the Fermi level allowing for *d*-to-*s* excitations to take place throughout the visible range.

The real part of the dielectric function (ε_1) describes the polarizability of the metal with respect to wavelength. It is generally negative for metals across a wide range of wavelengths as shown in Fig. 1a. From the data in Fig. 1a, it can be concluded that the first condition for plasmon excitation ($\varepsilon_1 \approx -2\varepsilon_m$) can be established for many metals in air at ultraviolet–visible wavelengths.

The imaginary part of the dielectric function (ε_2) is directly related to the probability of photon absorption (mainly through one-electron excitations) in the metal at a particular wavelength (Fig. 1b). There are two types of electronic excitations that can take place in these materials. It is possible to have electronic excitations from filled *s* states below the Fermi level to empty *s* states above the Fermi level, known as intraband excitations. These excitations are generally available for all transition metals in the visible range. The *s*-to-*s* excitations are indirect electronic excitations (that is, forbidden) that require the involvement of a third entity to provide the required change in the momentum of the charge carriers. This change in momentum can be supplied by lattice phonons, the nanoparticle surface or plasmons. Because these excitations require a third entity, intraband excitations exhibit a relatively small characteristic rate constant of ~10^{13} s^{-1} (ref. [39]). In addition to the *s*-to-*s* excitations, the excitations from filled *d* states below the Fermi level to empty *s* states above the Fermi level, known as interband excitations, can also take place. The availability of these transitions in the visible range for different metals depends on the location of the metal *d* states relative to the Fermi level. For instance, Ag is characterized by a full *d* band that lies well below the Fermi level (Fig. 1c). Consequently, *d*-to-*s* interband excitations cannot be induced by visible light photons in Ag. Au and Cu are also characterized by a full *d* band that lies below the Fermi level (Fig. 1c); however, the energy of the *d* band is higher compared with Ag, and visible light photons above a specific threshold energy are able to induce *d*-to-*s* interband excitations in these metals. In contrast to noble metals, the *d* states for the non-noble transition metals (Pt, Pd and so on) are not completely full and intersect the Fermi level (Fig. 1d). As a result, these metals can absorb photons via interband excitations throughout the visible range. In the case of the *d*-to-*s* interband excitations, no change in the momentum of the charge carriers is required, resulting in a larger characteristic rate constant for these excitations of ~10^{15} s^{-1} (ref. [39]). The difference in the inherent rates of the *s*-to-*s* compared with *d*-to-*s* excitations translates to higher values of ε_2 in the metals at the wavelength where the interband transitions are allowed. This means that non-noble metals have higher values of ε_2 compared with the noble metals at visible wavelengths. The data in Fig. 1b show that for visible wavelengths, ε_2 is small for Ag (across the entire visible range) as well as for Cu and Au above a threshold. The combination of $\varepsilon_1 \approx -2\varepsilon_m$ and low ε_2 stipulate that Ag, Au and Cu exhibit LSPR in the visible range. These metals are typically regarded as the plasmonic metals.

Characteristics of plasmon excitation. A direct consequence of plasmon excitation is the confinement of light energy near the surface of metal nanoparticles in the form of elevated electric fields[40]. The distribution of the confined electric fields in the metal is spatially inhomogeneous with the maximum field intensities localized at the surface of the nanoparticles[41]. The intensity of these fields decays dramatically with distance from the surface[42]. For isolated particles, the elevated field intensities can be up to 10^2 times the intensity of the incoming electromagnetic field and up to 10^3 times the intensity at corners or other sharp features of the nanoparticles[43]. Furthermore, the field confinement can reach 10^4–10^6 times the intensity of incoming radiation in the space between two closely positioned plasmonic nanoparticles. These regions of extremely high field intensities are commonly referred to as plasmonic hotspots. The amplification of the electric field intensity near the surface of the nanoparticles amplifies photophysical processes such as absorption (that is, excitation of energetic electron–hole pairs) and photon scattering, and it has been leveraged for applications in spectroscopy, chemical sensing and cancer therapy, among others[44–50]. A classic example of this is the amplification of inherently weak Raman scattering in surface-enhanced Raman spectroscopy[51–56].

The energy stored in the elevated LSPR fields is dissipated either through radiative photon scattering or nonradiative absorption in the metal nanoparticles within a very short time period, as the lifetime of a plasmonic excitation is in the femtosecond range[57–59]. Nonradiative absorption results in the generation of energetic charge carriers in the metal nanoparticles[60,61]. As discussed earlier, absorption (that is, the generation of energetic charge carriers) in metals can occur through either intraband *s*-to-*s* excitations or interband *d*-to-*s* excitations (Fig. 2a). Due to the inherently larger rate constant of interband excitations, plasmon decay via these excitations is the dominant decay pathway when available. Recent first principles calculations by Atwater et al. shed light on this phenomenon[62]. The data in Fig. 2b show the partitioning among various absorption pathways in plasmonic gold nanoparticles versus plasmon (photon) energy for different particle sizes. The data show that direct interband excitations are the dominant pathway for plasmon decay (photon absorption) in Au nanoparticles at energies where they are energetically accessible regardless of nanoparticle size. The contribution of the other absorption processes (that is, the phonon-assisted or surface-assisted intraband *s*-to-*s* excitations) are size dependent and only dominate for plasmon energies at which direct interband transitions are inaccessible[63,64].

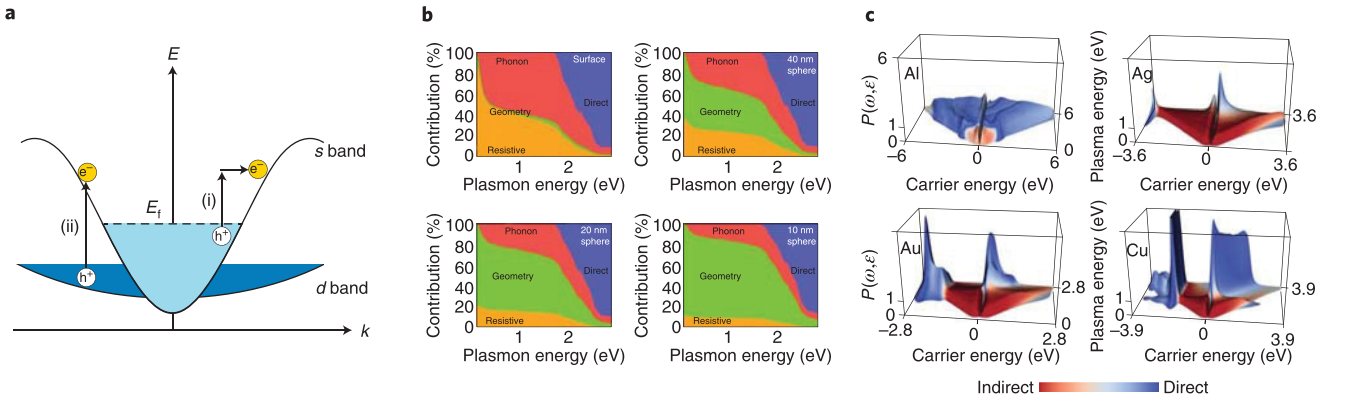

Fig. 2 | Plasmon decay through electronic excitations. a, Band diagram (energy (E) versus momentum (k)) depiction of photon absorption in metals through either *s*-to-*s* intraband excitations (i) or *d*-to-*s* interband excitations (ii). Intraband excitations require a change in momentum whereas interband excitations are direct electronic excitations, which do not require a change in momentum. **b**, Relative contributions of resistive, geometry-assisted, phonon-assisted and direct excitations to absorption in a semi-infinite gold surface and spherical gold nanoparticles of various sizes as a function of plasmon energy. Direct excitations in Au dominate when available regardless of the size of the Au particles. **c**, Energy distributions of initially excited hot carriers ($P(\omega,\varepsilon)$) in Al, Ag, Au and Cu as a function of plasmon frequency (ω) and carrier energy (ε). Excitation of intraband transitions results in the generation of equally energetic electrons and holes. Excitation of interband transitions generates an asymmetric distribution of low-energy electrons and high-energy holes. Panels adapted from: **a**, ref. [39], Springer Nature Ltd; **b**,**c**, ref. [62], American Chemical Society.

The pathway of plasmon decay governs the energy distribution of the initially excited hot charge carriers. It has been shown that the excitation of intraband transitions, which is the dominant plasmon decay absorption pathway in Ag at LSPR frequencies, results in the formation of hot electrons and holes in the *s* states of the metal that are of relatively equal energies, yielding a flat charge carrier distribution function (Fig. 2c)[62]. In contrast, excitation of interband transitions in Au and Cu results in an asymmetric initial energy distribution of energetic charge carriers wherein low-energy *s* electrons and high-energy *d* holes are produced (Fig. 2c). This distribution of energetic charge carriers is a direct consequence of exciting electrons from low-lying filled *d* states to empty *s* states above the Fermi level of these metals.

These initially formed high-energy charge carriers redistribute their energy through a number of relaxation processes. These relaxation processes are generally well understood[17,65]. The initially excited energetic charge carriers primarily redistribute energy through electron–electron collisions on the femtosecond timescale. This results in the secondary excitation of charge carriers near the Fermi level leading to a hot Fermi–Dirac distribution of energetic charge carriers on the approximately tens of femtoseconds timescale. These charge carriers further cool by coupling to phonon modes of the metal nanoparticles ultimately resulting in heating of the metals on the picosecond timescale. The energy is lost in the final process of energy exchange with the environment.

While the above-described relaxation processes and the dynamics of these processes have been illuminated mainly based on the behaviour of free electrons and holes (*s* band), there are no fundamental reasons to suggest that the lifetime of the *d* electrons or holes are significantly different. It has been suggested that hot *d* holes relax via an Auger process whereby an *s* electron fills the *d* hole creating an energetic *s* hole in the process[66]. This energetic *s* hole then relaxes via the electron–electron and electron–phonon interactions described above. Wolf and colleagues have suggested that this mechanism of energetic *d*-hole relaxation could slightly prolong the lifetime of energetic charge carriers in metals.

Activation of chemical bonds on plasmonic nanoparticles

When we entered this field, we postulated that the strong light–matter interaction displayed by plasmonic nanoparticles could result in surface chemical reactions. We demonstrated this by showing that partial oxidation reactions on plasmonic Ag nanoparticles can be induced by relatively low-intensity resonant light[25]. These initial studies were followed by an avalanche of reports of plasmon-driven reactions on Ag and Au nanoparticles[67–78]. For instance, plasmonic excitation of Ag and Au nanoparticles has been shown to activate CO oxidation, hydrogenation of carbonyls, dissociation of H_2 and reduction of nitroaromatics, among others[67–72]. We argued that the energy required to activate chemical bonds on the surfaces of plasmonic nanoparticles was provided by plasmon-mediated excitation of energetic charge carriers, which somehow end up in the reactants causing the reaction (Fig. 3a). We proposed this mechanism of bond activation (surface chemical transformation) on the plasmonic metal surfaces based on the above-mentioned studies of high-powered laser-induced reactions on bulk metal surfaces[21–24,79,80]. We note that the important difference here is that on the plasmonic nanoparticles, these reactions did not require high laser intensities. We come back to this point later. This transfer of energy to the molecule (reactant), in the form of hot charge or an electronic excitation, forces the molecule to evolve along a charged (or excited) potential energy surface, that is, the atoms of the molecule reconfigure to accommodate the potential energy surface. This molecular evolution can lead to a chemical transformation on the charged (or excited) potential energy surface, or once the charged (or excited) state decays, the molecule can return to the ground-state potential energy surface but with additional vibrational energy (Fig. 3a).

It is important to stress, as it is often misunderstood, that this process does not require charge extraction out of the metal (that is, the metal nanoparticle does not end up in a charged state). This process only leads to a transient electronic exchange between the metal and reactant (an electronic excitation in the adsorbate–metal complex), yielding transient adsorbate ions (or excited states localized on the reactant). These adsorbate ions survive on metal surfaces tens of femtoseconds before the relaxation, which is sufficient to induce chemical transformation or add vibrational energy to the reactant leading to the reaction. It is also important to stress that the lifetime of a vibrational excited molecule on metal surfaces is generally assumed to be in the picosecond range; however, a recent study by Wodtke et al. showed that in some cases, the vibrational lifetime extends to longer than 10^{-10} seconds[81]. We anticipate that this long lifetime of vibrational excited states might be a regular feature of weakly bonded molecules on Ag and Au as the energy

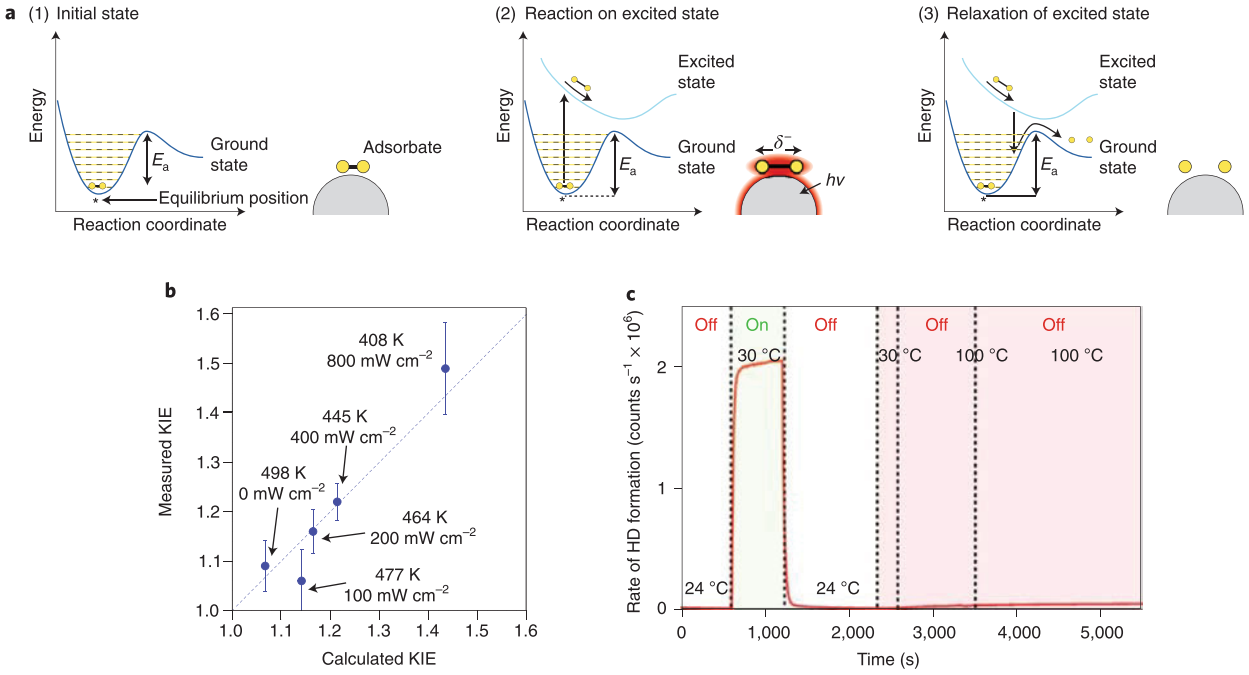

Fig. 3 | Mechanism of plasmon-mediated bond activation and evidence of charge-carrier-mediated reactions. a, Schematic of the desorption induced by electronic transitions mechanism for a dissociation reaction on a photoexcited plasmonic metal. (1) The adsorbate initially sits at the equilibrium position on its ground-state potential energy surface, requiring activation energy E_a to dissociate. (2) Photoexcitation of the plasmonic nanoparticle deposits plasmon energy into the adsorbate and elevates it to an excited potential energy surface. The adsorbate then moves along the excited potential energy surface, gaining kinetic energy and possibly reacting in the excited state. (3) If the adsorbate does not react in the excited state, it decays back down to the ground-state potential energy surface in a vibrationally excited state effectively lowering the barrier for dissociation. **b**, A parity plot of the calculated and experimentally measured KIE for oxygen dissociation on Ag nanocubes. The KIE is elevated under the influence of light. **c**, The photocatalytic rate of HD formation on Au nanoparticles compared with the purely thermal rate. It is clear that heating the catalyst to 100 °C results in a negligible increase of the rate compared with the photoexcited case at room temperature. Panels adapted from: **b**, ref. [67], Springer Nature Ltd; **c**, ref. [68], American Chemical Society.

dissipation pathways are more limited on these metals. This long lifetime would imply that a molecule can react on a metal surface in a vibrational hot state, that is, before it loses its vibrational energy to the surface. The above-described mechanism of bond activation, which involved electronic transitions, is known in the surface chemistry community as desorption induced by electronic transitions, where the reference to desorption comes from the fact that the initial reports of laser-induced surface chemistry were focused on desorption from metal surfaces[79].

These charge-carrier-driven reactions on metals exhibit a few unique experimental signatures compared with thermal reactions[23,67]. A classic signature of the charge-carrier-mediated reactions on metals that involve electronically excited states, suggested based on the laser-induced chemistry experiments on extended metal surfaces, is an elevated primary kinetic isotope effect (KIE) compared with the KIE associated with the thermal reaction[23,79].

Motivated by seeking to demonstrate that the light-driven reactions on metals were indeed driven by energetic charge carriers, our group examined the KIE for the dissociation of O_2 on plasmonic Ag nanoparticles[25,67]. We hypothesized that plasmon-excited energetic charge carriers drive dissociation of O_2 on the photoexcited Ag nanoparticles. We performed reactor experiments for O_2 dissociation on plasmonic Ag using $^{16}O_2$ and $^{18}O_2$ under purely thermal conditions and under illumination. The KIE for both experiments were computed by taking the ratio of the $^{16}O_2$ reaction rate to the $^{18}O_2$ reaction rate. The results from the KIE experiments are shown in Fig. 3b. Under purely thermal conditions, a KIE of 1.06 was measured. However, photoexcitation of the plasmonic catalyst resulted in an elevated KIE of up to 1.48. This stark contrast in the observed KIE supports the conclusion that O_2 dissociation under photoexcitation was aided by plasmon-induced excitation of energetic charge carriers.

These findings of charge carrier-mediated reactions on photoexcited plasmonic catalysts were corroborated by several other groups for a number of different chemical transformations on Ag and Au nanoparticles. For example, Halas et al. demonstrated that photoexcited Au nanoparticles catalysed the dissociation of H_2 at room temperature whereas little-to-no dissociation took place under purely thermal conditions even at temperatures as high as 100 °C (Fig. 3c)[26,68]. Furthermore, it was shown that the photocatalytic rate of H_2 dissociation was proportional to the plasmon intensity of the Au nanoparticles, which demonstrated that plasmon-mediated excitation of energetic charge carriers was involved in the activation of H_2 on the Au nanoparticles. In a separate case, Moores et al. showed that plasmonic Ag nanoparticles could drive photocatalytic hydrogenation of carbonyls under plasmon excitation[69]. Here again, no chemical conversion was observed under purely thermal conditions, suggesting that the reaction was driven by plasmon-derived energetic charge carriers.

These initial mechanistic findings of charge-carrier-mediated reactions on photoexcited plasmonic nanoparticles inspired further interest in this field as it offered opportunities to move away from reaction outcomes (selectivity) induced by thermal fluxes and potentially develop more selective catalytic processes. As we mentioned above, in temperature-driven reactions, energy is provided to all available degrees of freedom (all vibrational, rotational and translational modes) resulting in the simultaneous activation of many reaction pathways. Alternatively, charge-carrier-mediated reactions potentially offer the opportunity to push the evolution of

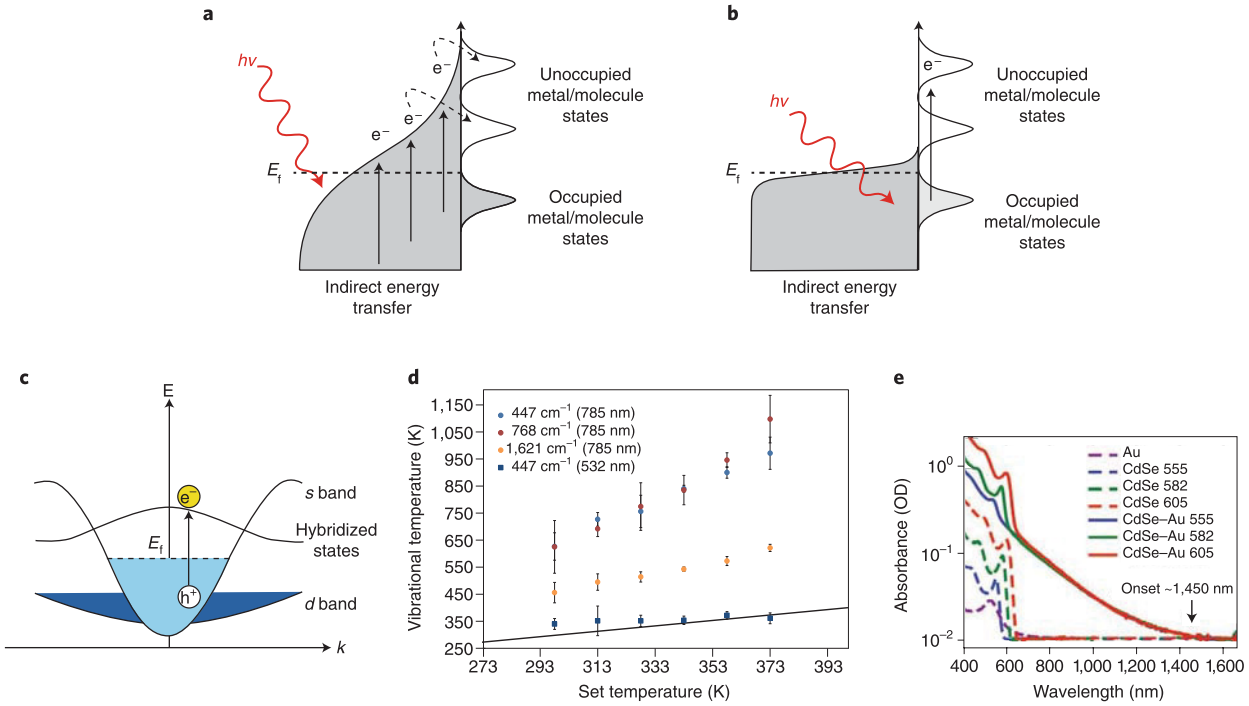

Fig. 4 | Mechanisms of plasmon-mediated energy transfer to reactants. a, Indirect energy transfer mechanism. Plasmon relaxation results in an electron distribution that is characterized by a high concentration of low-energy charge carriers. Charge carriers with adequate energy can transfer to metal–adsorbate states at the interface. **b**, Direct energy transfer mechanism. Plasmon decay results in the direct excitation of charge carriers to states of the adsorbate–metal complex at the interface. **c**, A band structure representation of the direct energy transfer mechanism. The adsorption of molecules on the metal surface create new metal–molecule states at the interface that can allow for direct, momentum-conserved electronic excitations between the metal and these new states. **d**, Temperatures of different vibrational modes of MB adsorbed on Ag. Under 532 nm illumination, the vibrational temperature is nearly equal to the set temperature (represented by the black line). Under 785 nm illumination, the vibrational temperatures for all modes are significantly increased above the metal nanoparticle temperature, indicating a resonant, selective energy transfer into the MB adsorbate. **e**, Excitation of Au nanoparticles strongly coupled with CdSe nanorods causes plasmon decay by directly creating an electron in the conduction band of the semiconductor and a hole in the metal, which results in a damped SPR band of the Au nanoparticles and a continuous absorption feature extending to the near-infrared spectrum. Panels adapted with permission from: **d**, ref. [86], American Chemical Society; **e**, ref. [88], AAAS.

reactants to a desired product state by selectively depositing energy in a particular reaction coordinate (for example, a particular vibrational mode through the above-described hot-electron heating)[28,82].

Transient electronic excitations into reactants

While many groups focused on demonstrating plasmonic chemistry for different chemical transformations, we decided to spend considerable time attempting to understand the mechanism that leads to the electronic excitations in the adsorbate–metal complexes, that is, how an energetic carrier finds its way to the reactant. Our motivation for focusing on this question came from the simple observation that the above-mentioned photoinduced reactions on extended, bulk metal surfaces required significantly higher light intensity compared with the reactions on plasmonic metal nanoparticles. While some of this difference arises from the significantly larger optical cross-sections and surface-to-volume ratios of plasmonic metal nanoparticles compared with extended metal surfaces, it was clear that there might be additional factors that allowed plasmonic nanoparticles to be significantly more efficient.

The accepted mechanism of energy transfer from metals to adsorbates, which was observed on extended metal surfaces illuminated by high-intensity lasers, is termed the indirect mechanism. It assumes that photon absorption results in the generation of energetic charge carriers within the metal followed by charge injection into accessible adsorbate orbitals. We postulated that in the plasmonic metal nanoparticles, an alternative direct mechanism might play an important role. Under this mechanism plasmon decay results in direct electronic excitations at the adsorbate or at the adsorbate/metal interface. This effectively means that the fundamental photophysical process underlying the plasmonic chemistry is different than the one underlying the chemistry on extended metal surfaces. We discuss both mechanisms in more detail in the following sections.

Indirect transfer of energy. In this mechanism, photoexcitation of the plasmonic metals results in the excitation of energetic charge carriers in the metal nanoparticle as discussed above. These charge carriers then collide with other charge carriers forming an energized (hot) Fermi–Dirac distribution. Energetic charge carriers from this distribution can transfer from the metal to unpopulated states (orbitals) at the adsorbate (Fig. 4a).

In this mechanism, the transfer of energetic charge carriers to adsorbates will depend on the positioning of the adsorbate states relative to the Fermi level of the metal. Since the Fermi–Dirac distribution is characterized by an elevated concentration of hot carriers close to the Fermi level, the adsorbate states closer to the Fermi level will always experience higher rates of energy transfer. Although this energy transfer mechanism could in principle produce reaction outcomes unique from thermal reactions, it does not allow for significant control of the energy transfer process (that is, ability to target particular orbitals), which ultimately limits the ability to control product selectivity.

Direct transfer of energy. We postulated that in plasmonic nanoparticles, the indirect mechanism, while potentially important,

was not the only way by which plasmonic energy was transferred to the reactants. We hypothesized an alternative mechanism that involved the direct excitation of charge carriers within the metal–reactant complex at the adsorbate/metal interface, as depicted in Fig. 4b[83,84]. In this mechanism, interactions between the adsorbate and the metal result in the evolution of electronic states at the interface. These interfacial electronic states provide an additional energy dissipation pathway for the energy collected via LSPR excitation through direct momentum-conserved excitations of electrons involving these states (Fig. 4c)[85]. In contrast to the indirect mechanism, the direct mechanism avoids the excitation of charge carriers in the metal, suggesting that plasmon energy can be channelled to particular adsorbates by targeting specific states at the interface with resonant photons.

We demonstrated the existence of the direct charge excitation mechanism as an important pathway for energy transfer to adsorbates in a case study of methylene blue (MB) chemisorbed on Ag nanoparticles[83,86]. In this study, we used LSPR-enhanced Raman spectroscopy (essentially surface-enhanced Raman spectroscopy) to probe the energy transfer between plasmonic Ag and MB molecules attached to Ag. It is well-established that charge excitation in an attached molecule (in this case MB) or transfer of energetic charge carriers to the molecule leads to vibrational heating of the molecule[54,87]. This can be measured by comparing the intensities of the anti-Stokes and Stokes Raman scattering processes. We found that the photoexcitation of the system with a 785 nm Raman laser resulted in significantly more energy transfer to the MB molecule compared with photoexcitation with 532 nm light of the same photon flux. This resonant energy transfer induced by 785 nm photons resulted in the non-equilibrium heating of the molecule, compared with the Ag substrate, as shown in Fig. 4d. The non-equilibrium heating of the molecule was not observed for the 532 nm laser[83,86]. The results suggested that the interaction of the adsorbate with the metal nanoparticles opened new channels for energy dissipation that could be induced using 785 nm light but were inaccessible to 532 nm light. Based on these findings, we suggested a resonant flow of energy involving direct electronic excitations at the MB/Ag interface.

Similar findings demonstrating the importance of interfacial states on the flow of LSPR energy were reported in a few other studies that relied on variations of pump and probe measurements[88–91]. For example, Lian et al. argued that the chemical attachment of Au nanoparticles to CdSe nanorods resulted in strong mixing of the electronic states of the two materials[88]. This interaction opened a new, very fast pathway for the dissipation of plasmon energy via interfacial charge carrier excitations. Optical measurements combined with transient absorption spectroscopy (Fig. 4e) demonstrated that plasmon excitation of the Au nanoparticles resulted in energy transfer to the CdSe nanorods via direct electronic transitions from filled metal states to the conduction band of the semiconductor at the interface between the two materials. Similarly, Petek et al. applied ultrafast two-photon photoemission spectroscopy to demonstrate the emergence of a direct charge excitation pathway across a Ag/TiO_2 heterojunction[89]. The photoexcitation of the Ag/TiO_2 heterojunction resulted in dephasing of the plasmon excitation in Ag, which generated hot electrons with anisotropic and non-thermal distributions in TiO_2 near the metal/semiconductor interface. Furthermore, time-resolved measurements showed ultrafast relaxation (<10 fs) of the hot electrons consistent with direct excitations taking place between Ag and TiO_2, rather than by excitations in Ag followed by charge injection into TiO_2. Another recent study by Kazuma et al. reported on the real-time observation of the plasmon-induced dissociation of dimethyl disulfide via a direct excitation mechanism using scanning tunnelling microscopy[90]. It was argued that the intense fields generated between a Ag scanning tunnelling microscope tip and a metal substrate (where the probe molecules were located) facilitated the dissociation via direct excitations at the interface. Wavelength-dependent measurements of the LSPR-induced dissociation rate (when the field is present) and the photoinduced dissociation rate (when the dissociation is triggered by tunnelling electrons) demonstrated that the plasmon-generated fields promoted direct excitations at the interface and dissociation of the molecules.

This direct mechanism of energy transfer is in line with previously suggested chemical interface damping of plasmons[92–95]. The advancement made by recent contributions is that previously we had no clear models that shed light on when this mechanism of LSPR-energy transfer was functional and therefore no clear understanding of how to take advantage of these physical processes. Based on our work on various probe molecules (including the above-mentioned MB), we proposed that there were at least two critical requirements for the exchange of energy between plasmonic nanostructures and reactants[83,86]. One requirement is the intense electric field generated at the surface via LSPR excitation that essentially reroutes charge excitation processes to the surface. The second requirement is the existence of the electronic states at the surface that allow for inherently fast, momentum-conserved direct electronic excitations at the locations where the LSPR field intensities are high.

Multicomponent plasmonic catalysts. This understanding of the mechanisms associated with the energy flow in plasmonic catalysis provided us with a framework for integrating plasmonic nanostructures with other non-plasmonic materials into multicomponent plasmonic catalysts. In particular, we were interested in designing hybrid plasmonic–catalytic materials where the energy harvested by the plasmonic particle is efficiently transferred to a different catalytic material where chemical transformations can take place. This development of multicomponent plasmonic catalysts is critical due to the limited catalytic activity of plasmonic metals (Cu, Ag and Au), which constrains the phase space of reactions that could be activated using these strategies.

Based on the proposed direct mechanism of energy transfer, we hypothesized that the energy of light concentrated through LSPR excitation in a plasmonic nanoparticle could be transferred to a catalytic material, attached to the nanoparticle, via LSPR-induced direct electronic excitations in the catalytic material. In the case of catalytically active metals, this hypothesis relied on the fact that the electronic structure of most catalytic metals (Pt, Pd, Ru and so on) feature *d* bands at the Fermi level, which allow for direct, momentum-conserved interband excitations in the visible range. We postulated that this enables catalytic metals to act as absorption sinks for the electromagnetic energy concentrated by plasmonic metals.

We recently tested this hypothesis in a bimetallic model system composed of a relatively large Ag nanocube core (75 nm) surrounded by a thin ~1 nm shell of Pt (Fig. 5a)[96]. Measurements of the optical properties of monometallic Ag nanocubes showed that plasmon decay primarily resulted in photon scattering. However, coating the Ag nanocubes with a 1-nm-thick shell of Pt resulted in a drastic change in the plasmon decay pathway where absorption was now strongly favoured over scattering (Fig. 5b). These data suggested that the thin Pt at the surface was providing an efficient pathway for the dissipation of plasmonic energy thereby redirecting plasmon energy to the thin Pt shell. The spatial distribution of the LSPR energy dissipation was modelled using electrodynamic simulations. The simulation data showed that the majority of the absorption in the particle was taking place in the thin Pt shell (Fig. 5c). These hybrid plasmonic–catalytic nanoparticles were then used to perform plasmon-enhanced preferential CO oxidation in excess H_2. The reactor experiments demonstrated that the charge carriers produced in the Pt shell by LSPR excitation from the Ag core could be used to perform Pt surface chemistry.

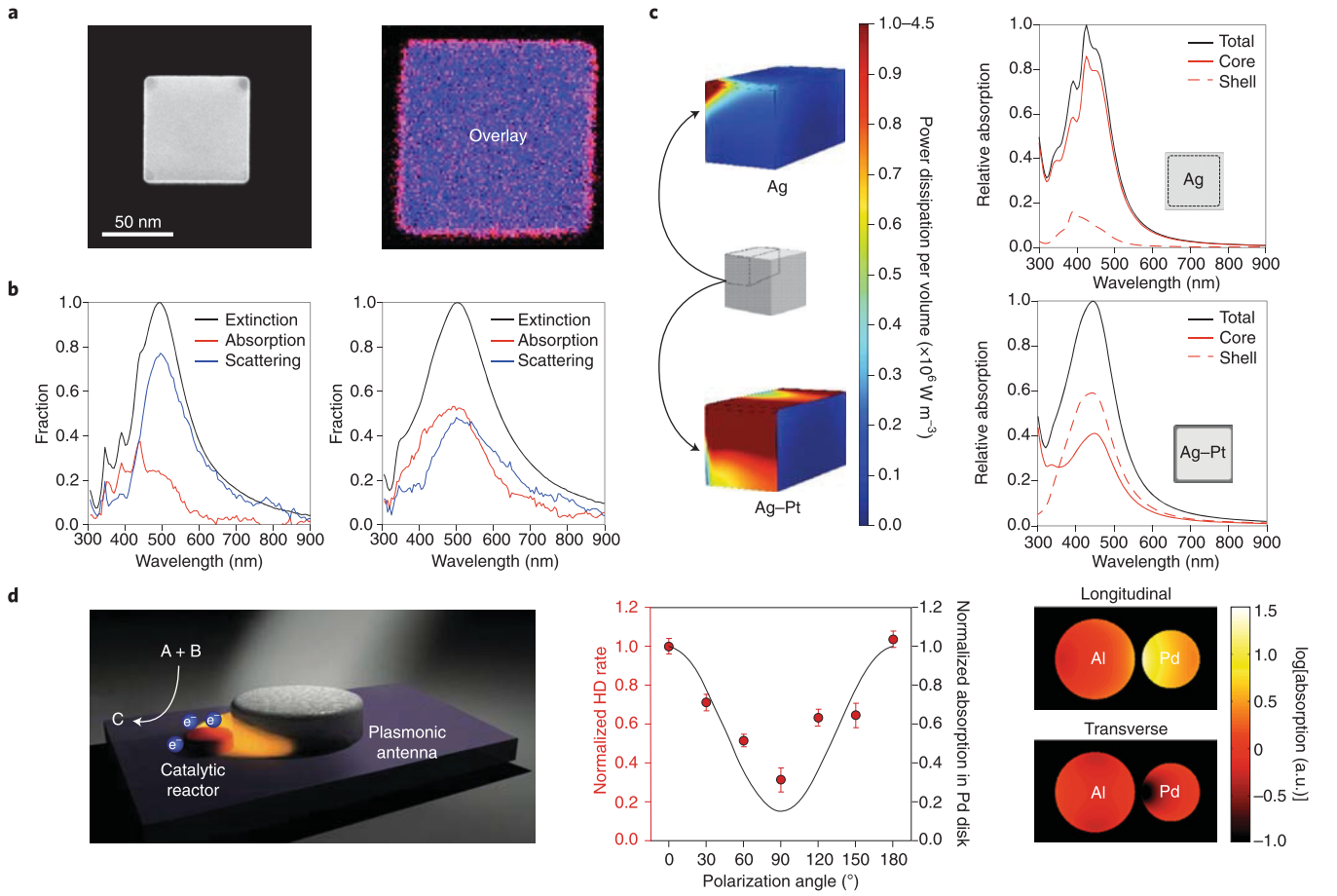

Fig. 5 | Multicomponent plasmonic catalysts. a, Dark-field scanning transmission electron microscopy image (left) and energy-dispersive X-ray spectroscopy elemental map (right) of a Ag–Pt core–shell nanocube showing distributions of Ag (blue) and Pt (red). **b**, Extinction, absorption and scattering spectra of Ag (left) and Ag–Pt nanocubes (right). The absorption-to-scattering ratio is drastically altered in favour of absorption when the Ag nanocube is coated with ~1 nm of Pt. **c**, Simulated power dissipated through Ag and Ag–Pt nanocubes. Left: contour map of power dissipated through a Ag (upper) or Ag–Pt (lower) nanocube. The thin coating of Pt strongly biases energy dissipation through the nanoparticle shell. Right: simulated light absorption in the core versus the outermost layers of a Ag nanocube (top) and a Ag–Pt nanocube (bottom). In the pure Ag nanocube, nearly all the absorption takes place in the core of the nanoparticle. In contrast, the thin coating of Pt re-routes the flow of energy so that most of the absorption takes place in the thin ~1 nm shell of Pt. **d**, Studies of antenna reactor systems. Left: schematic of the bimetallic antenna–reactor system. Middle: normalized rate of HD production on Al–Pd heterodimers and absorption in the Pd disk as a function of light polarization. Right: simulated absorption maps in the Al–Pd heterodimers. Collectively, the data show that reaction rate and absorption in Pd are the highest when the plasmon-induced electric fields are the highest. Panels reproduced from: **a**–**c**, ref. [96], Springer Nature Ltd; **d**, ref. [97], AAAS (left); ref. [98], American Chemical Society (middle and right).

Similar to our work, Halas and colleagues demonstrated the design of antenna–reactor systems in which a plasmonic metal (that is, the antenna) acts to collect and concentrate visible light energy and transfer that energy to a catalytic metal (that is, the reactor) where it is used to drive a chemical reaction (Fig. 5d)[97,98]. This concept was demonstrated using Al surrounded by a thin layer of Al_2O_3 as a plasmonic antenna and Pd nanoparticles as catalytic reactors to drive photocatalytic reduction of acetylene and dissociation of H_2. Because the Pd nanoparticles were not in direct contact with the plasmonic Al, it was argued that the energy transfer resulting in increased reaction rates could only take place via a field effect where the field from the plasmonic Al was felt by the catalytic Pd nanoparticles resulting in the excitation of charge carriers in Pd.

We have also recently investigated this energy transfer mechanism in more detail. From this work, it is clear that the two main requirements for energy transfer are (1) high electric field intensities provided by LSPR excitation of plasmonic metals and (2) the availability of direct, momentum-conserved electronic transitions in the catalytic material at the LSPR excitation frequencies. By positioning the catalytic material at the positions where the electric field intensities are the highest (that is, at the surface of the plasmonic metal), the energy transfer from the plasmonic metal to the catalytic metal can be maximized. A crucial feature of this mechanism is that it avoids, to a large extent, the loss of energy via absorption in the plasmonic metal allowing for high-energy carriers to be generated directly in the catalytic metal. The understanding of this mechanism now allows for the conceptualization of new designs of hybrid plasmonic–catalytic metal nanoparticles for performing chemical reactions beyond those for which only Ag and Au are catalytically active.

Current trends and outlook

In our discussions above, we have mainly focused on discussing plasmonic chemical transformations that involve one-electron (one-hole) or one electronic excitation process. We have discussed these reactions in the context of a transient charge excitation within the metal–reactant complex, where this excitation results in energy transfer into the reaction coordinate. The mechanism we discussed does not require multiple electronic excitations, a long lifetime

of the electronic excitation or charge extraction from the metal nanoparticle. This mechanism allows for the plasmonic acceleration of processes that already take place thermally or potentially for an activation of alternative chemical routes (different product selectivity compared with the thermal process) via the direct mechanism of energy exchange between a plasmonic structure and an adsorbate.

There have been a number of recent reports of multi-electron (or -hole) reactions, such as CO_2 or N_2 reduction, on plasmonic nanoparticles, akin to the processes that could take place on semiconductor light absorbers or in electrochemical systems. Although this idea is intriguing, there are several potential issues that need to be addressed, understood and explained. First, these multi-electron processes have been observed mainly when charge scavengers have been employed, so to fully understand these process it is critical to: (1) establish that the products are actually derived from the reactants (N_2 or CO_2) rather than from the scavengers or impurities, (2) evaluate the quantum efficiencies in terms of the reaction rates obtained and the light intensity used in the experiments — very low rates or large intensity requirements would be discouraging in this context — and (3) critically assess the overall thermodynamic efficiencies of these processes as these processes often employ high-energy scavenger molecules. The promise of solar-to-chemical energy conversion (CO_2 or N_2 reduction) rests on the ability to use sunlight to power endothermic processes, and for these particular reactions, it implies that the reducing hydrogen molecules are derived from water and not from a scavenger. Furthermore, to execute these multi-electron reactions, multiple electrons (or holes) need to transfer to reaction intermediates quite rapidly. This rapid transfer is required as the reaction intermediates are unstable and the reverse reactions are thermodynamically preferred. In highly endothermic reactions (H_2O splitting or CO_2 reduction that uses water as the source of hydrogen), the energy of these charge carriers also needs to be high. In electrochemical metallic systems, execution of these multi-electron reactions requires changing the voltage of the metal, thereby lifting the energy of every charge carrier in the metal. This ensures that the electrochemical potential of the charge carriers is sufficiently high to allow for a rapid transfer to the reactants. This often leads to high electrochemical losses (overpotential) associated with these reactions. As discussed earlier, in plasmonic nanostructures single-electron excitations take place, the lifetime of photogenerated high-energy charge carriers in metals is short (approximately tens of femtoseconds), and the time between excitation events is relatively long at low light intensities (for example, one Sun). Given these physical constraints, it is difficult to argue that multiple electronic excitations, required to execute multi-electron reactions, can take place faster than the reverse reactions. Therefore, in our view different mechanistic explanations are required to explain the observations of plasmon-driven multi-electron (-hole) reactions. The central question is how can multiple high-energy charge carriers be supplied to the high-energy intermediates in short times under moderate light intensities (sunlight) without the aid of high energy scavengers?

Ultimately, the promise of plasmonic catalysis rests on the ability to perform surface chemistry with higher control over the product selectivity than in purely temperature-driven chemical reactions. The above-described experimental observations and models supporting the direct energy transfer mechanism imply that it is in principle possible to selectively excite specific electronic excitations at the molecule/nanoparticle interface. Whether these excitations yield a preferential heating of specific vibrational modes is ultimately related to the distribution of this electronic energy among different vibrational modes, which is in turn governed by the shape of the excited potential energy surface (that is, the transient ion potential energy surface). Clearly, engineering selective chemistry will require engineering of not only optical properties of the plasmonic metal, but also the electronic structure of the reactants adsorbed on the active centres as well as the ground and excited potential energy surfaces. In principle, this will require a complete, almost atomistic control over the entire multifunctional plasmonic catalyst. Quantum chemical calculations can be very helpful in identifying the desired structures and potentially guiding us in the discovery of selective plasmonic catalysts[99,100].

As the field of plasmonic catalysis continues to grow, it is becoming ever more important to avoid missteps that could lead the field in wrong directions or overpromise and underdeliver. For instance, it is not uncommon to see optical and catalytic data exaggerated or incorrectly interpreted to support certain claims in the literature. Similarly, claims about physical phenomena are often presented without providing the appropriate data to support them. These practices, although common in emerging fields, hinder progress and hopefully will be minimized and avoided. Nevertheless, plasmonic catalysis has seen significant growth over the past few years. With continued progress in the areas of quantum chemistry and precision synthesis of nanomaterials, we anticipate the field will experience significant advancements in the coming years.

Received: 1 June 2018; Accepted: 1 August 2018;
Published online: 12 September 2018

References

1. Ertl, G. Reactions at surfaces: from atoms to complexity (Nobel Lecture). *Angew. Chem. Int. Ed.* **47**, 3524–3535 (2008).
2. Hinrichsen, O., Rosowski, F., Hornung, A., Muhler, M. & Ertl, G. The kinetics of ammonia synthesis over Ru-based catalysts: 1. The dissociative chemisorption and associative desorption of N_2. *J. Catal.* **165**, 33–44 (1997).
3. Haryanto, A., Fernando, S., Murali, N. & Adhikari, S. Current status of hydrogen production techniques by steam reforming of ethanol: a review. *Energy Fuels* **19**, 2098–2106 (2005).
4. Nikolla, E., Holewinski, A., Schwank, J. & Linic, S. Controlling carbon surface chemistry by alloying: carbon tolerant reforming catalyst. *J. Am. Chem. Soc.* **128**, 11354–11355 (2006).
5. Studt, F. et al. Identification of non-precious metal alloy catalysts for selective hydrogenation of acetylene. *Science* **320**, 1320–1322 (2008).
6. Kliewer, C. J., Bieri, M. & Somorjai, G. A. Hydrogenation of the α,β -unsaturated aldehydes acrolein, crotonaldehyde, and prenal over Pt single crystals: a kinetic and sum-frequency generation vibrational spectroscopy study. *J. Am. Chem. Soc.* **131**, 9958–9966 (2009).
7. Saavedra, J. et al. Controlling activity and selectivity using water in the Au-catalysed preferential oxidation of CO in H_2. *Nat. Chem.* **8**, 584–589 (2016).
8. Dellamorte, J. C., Lauterbach, J. & Barteau, M. A. Palladium–silver bimetallic catalysts with improved activity and selectivity for ethylene epoxidation. *Appl. Catal. Gen.* **391**, 281–288 (2011).
9. Grabow, L. C., Gokhale, A. A., Evans, S. T., Dumesic, J. A. & Mavrikakis, M. Mechanism of the water gas shift reaction on Pt: first principles, experiments, and microkinetic modeling. *J. Phys. Chem. C* **112**, 4608–4617 (2008).
10. Stamenkovic, V. R. et al. Improved oxygen reduction activity on $Pt_3Ni(111)$ via increased surface site availability. *Science* **315**, 493–497 (2007).
11. Cleve, T. V., Moniri, S., Belok, G., More, K. L. & Linic, S. Nanoscale engineering of efficient oxygen reduction electrocatalysts by tailoring the local chemical environment of Pt surface sites. *ACS Catal.* **7**, 17–24 (2017).
12. Hu, B. et al. Selective propane dehydrogenation with single-site Co^{II} on SiO_2 by a non-redox mechanism. *J. Catal.* **322**, 24–37 (2015).
13. Christopher, P. & Linic, S. Shape- and size-specific chemistry of Ag nanostructures in catalytic ethylene epoxidation. *ChemCatChem* **2**, 78–83 (2010).
14. Holewinski, A., Xin, H., Nikolla, E. & Linic, S. Identifying optimal active sites for heterogeneous catalysis by metal alloys based on molecular descriptors and electronic structure engineering. *Curr. Opin. Chem. Eng.* **2**, 312–319 (2013).
15. Schweitzer, N., Xin, H., Nikolla, E., Miller, J. T. & Linic, S. Establishing relationships between the geometric structure and chemical reactivity of alloy catalysts based on their measured electronic structure. *Top. Catal.* **53**, 348–356 (2010).
16. Lindstrom, C. D. & Zhu, X.-Y. Photoinduced electron transfer at molecule–metal interfaces. *Chem. Rev.* **106**, 4281–4300 (2006).
Review paper summarizing mechanisms of electron transfer at molecule–metal interfaces with emphasis on the role of chemical bonding at the interface.

17. Frischkorn, C. & Wolf, M. Femtochemistry at metal surfaces: nonadiabatic reaction dynamics. *Chem. Rev.* **106**, 4207–4233 (2006).
18. White, J. M. Using photons and electrons to drive surface chemical reactions. *J. Mol. Catal. Chem.* **131**, 71–90 (1998).
19. Busch, D. G. & Ho, W. Direct observation of the crossover from single to multiple excitations in femtosecond surface photochemistry. *Phys. Rev. Lett.* **77**, 1338–1341 (1996).
20. Linic, S., Christopher, P., Xin, H. & Marimuthu, A. Catalytic and photocatalytic transformations on metal nanoparticles with targeted geometric and plasmonic properties. *Acc. Chem. Res.* **46**, 1890–1899 (2013).
21. Buntin, S., Richter, L., Cavanagh, R. & King, D. Optically driven surface reactions: evidence for the role of hot electrons. *Phys. Rev. Lett.* **61**, 1321–1324 (1988).
22. Deliwala, S. et al. Surface femtochemistry of O_2 and CO on Pt(111). *Chem. Phys. Lett.* **242**, 617–622 (1995).
23. Bonn, M. et al. Phonon- versus electron-mediated desorption and oxidation of CO on Ru(0001). *Science* **285**, 1042–1045 (1999).
Demonstration of unique chemical reaction outcomes for electron-mediated processes versus phonon-mediated processes on bulk metals under laser excitation.
24. Hertel, T., Knoesel, E., Wolf, M. & Ertl, G. Ultrafast electron dynamics at Cu(111): response of an electron gas to optical excitation. *Phys. Rev. Lett.* **76**, 535–538 (1996).
25. Christopher, P., Xin, H. & Linic, S. Visible-light-enhanced catalytic oxidation reactions on plasmonic silver nanostructures. *Nat. Chem.* **3**, 467–472 (2011).
Demonstration of visible-light-enhanced reactions on plasmonic Ag nanostructures with systematic experiments uncovering the role of hot charge carriers in activating chemical bonds.
26. Mukherjee, S. et al. Hot electrons do the impossible: plasmon-induced dissociation of H_2 on Au. *Nano Lett.* **13**, 240–247 (2013).
27. Marimuthu, A., Zhang, J. & Linic, S. Tuning selectivity in propylene epoxidation by plasmon mediated photo-switching of Cu oxidation state. *Science* **339**, 1590–1593 (2013).
A unique case in which plasmon excitation causes a change in the oxidation state of a metal catalyst under operating conditions resulting in a significant improvement of product selectivity.
28. Linic, S., Aslam, U., Boerigter, C. & Morabito, M. Photochemical transformations on plasmonic metal nanoparticles. *Nat. Mater.* **14**, 567–576 (2015).
29. Kale, M. J., Avanesian, T. & Christopher, P. Direct photocatalysis by plasmonic nanostructures. *ACS Catal.* **4**, 116–128 (2014).
30. Zhang, Y. et al. Surface-plasmon-driven hot electron photochemistry. *Chem. Rev.* **118**, 2927–2954 (2018).
31. Zhang, X., Chen, Y. L., Liu, R.-S. & Tsai, D. P. Plasmonic photocatalysis. *Rep. Prog. Phys.* **76**, 046401 (2013).
32. Maier, S. A. *Plasmonics: Fundamentals and Applications* (Springer Science and Business Media, Bath, 2007).
33. Kelly, K. L., Coronado, E., Zhao, L. L. & Schatz, G. C. The optical properties of metal nanoparticles: the influence of size, shape, and dielectric environment. *J. Phys. Chem. B* **107**, 668–677 (2002).
34. Link, S. & El-Sayed, M. A. Spectral properties and relaxation dynamics of surface plasmon electronic oscillations in gold and silver nanodots and nanorods. *J. Phys. Chem. B* **103**, 8410–8426 (1999).
35. El-Sayed, M. A. Some interesting properties of metals confined in time and nanometer space of different shapes. *Acc. Chem. Res.* **34**, 257–264 (2001).
36. Langhammer, C., Kasemo, B. & Zorić, I. Absorption and scattering of light by Pt, Pd, Ag, and Au nanodisks: absolute cross sections and branching ratios. *J. Chem. Phys.* **126**, 194702 (2007).
37. Kreibig, U. & Vollmer, M. *Optical Properties of Metal Clusters* (Springer Science and Business Media, Heidelberg, 2013).
Provides a comprehensive introduction to plasmonic excitation in metal nanoparticles.
38. Stiles, P. L., Dieringer, J. A., Shah, N. C. & Duyne, R. P. V. Surface-enhanced raman spectroscopy. *Annu. Rev. Anal. Chem.* **1**, 601–626 (2008).
39. Khurgin, J. B. How to deal with the loss in plasmonics and metamaterials. *Nat. Nanotech.* **10**, 2–6 (2015).
40. Halas, N. J., Lal, S., Chang, W.-S., Link, S. & Nordlander, P. Plasmons in strongly coupled metallic nanostructures. *Chem. Rev.* **111**, 3913–3961 (2011).
41. Hao, E. & Schatz, G. C. Electromagnetic fields around silver nanoparticles and dimers. *J. Chem. Phys.* **120**, 357–366 (2004).
42. Ingram, D. B. & Linic, S. Water splitting on composite plasmonic-metal/semiconductor photoelectrodes: evidence for selective plasmon-induced formation of charge carriers near the semiconductor surface. *J. Am. Chem. Soc.* **133**, 5202–5205 (2011).
43. Linic, S., Christopher, P. & Ingram, D. B. Plasmonic-metal nanostructures for efficient conversion of solar to chemical energy. *Nat. Mater.* **10**, 911–921 (2011).
44. Kambhampati, P., Child, C. M., Foster, M. C. & Campion, A. On the chemical mechanism of surface enhanced Raman scattering: experiment and theory. *J. Chem. Phys.* **108**, 5013–5026 (1998).
45. Jain, P. K., Huang, X., El-Sayed, I. H. & El-Sayed, M. A. Noble metals on the nanoscale: optical and photothermal properties and some applications in imaging, sensing, biology, and medicine. *Acc. Chem. Res.* **41**, 1578–1586 (2008).
46. Dolinnyi, A. I. Nanometric rulers based on plasmon coupling in pairs of gold nanoparticles. *J. Phys. Chem. C* **119**, 4990–5001 (2015).
47. Nasir, M. E., Dickson, W., Wurtz, G. A., Wardley, W. P. & Zayats, A. V. Hydrogen detected by the naked eye: optical hydrogen gas sensors based on core/shell plasmonic nanorod metamaterials. *Adv. Mater.* **26**, 3532–3537 (2014).
48. Carpin, L. B. et al. Immunoconjugated gold nanoshell-mediated photothermal ablation of trastuzumab-resistant breast cancer cells. *Breast Cancer Res. Treat.* **125**, 27–34 (2010).
49. El-Sayed, I. H., Huang, X. & El-Sayed, M. A. Selective laser photo-thermal therapy of epithelial carcinoma using anti-EGFR antibody conjugated gold nanoparticles. *Cancer Lett.* **239**, 129–135 (2006).
50. Neumann, O. et al. Nanoparticle-mediated, light-induced phase separations. *Nano Lett.* **15**, 7880–7885 (2015).
51. Brus, L. Noble metal nanocrystals: plasmon electron transfer photochemistry and single-molecule Raman spectroscopy. *Acc. Chem. Res.* **41**, 1742–1749 (2008).
Article highlighting strong light–matter interactions among plasmonic nanostructures and molecules.
52. Moskovits, M. Surface-enhanced spectroscopy. *Rev. Mod. Phys.* **57**, 783–826 (1985).
53. Moskovits, M. Surface-enhanced Raman spectroscopy: a brief retrospective. *J. Raman Spectrosc.* **36**, 485–496 (2005).
54. Kneipp, K. et al. Near-infrared surface-enhanced Raman scattering can detect single molecules and observe 'hot' vibrational transitions. *J. Raman Spectrosc.* **29**, 743–747 (1998).
55. Jiang, Bosnick, K., Maillard, M. & Brus, L. Single molecule Raman spectroscopy at the junctions of large Ag nanocrystals. *J. Phys. Chem. B* **107**, 9964–9972 (2003).
56. Kneipp, K. et al. Single molecule detection using surface-enhanced Raman scattering (SERS). *Phys. Rev. Lett.* **78**, 1667–1670 (1997).
57. Evanoff, D. D. & Chumanov, G. Size-controlled synthesis of nanoparticles. 2. Measurement of extinction, scattering, and absorption cross sections. *J. Phys. Chem. B* **108**, 13957–13962 (2004).
58. Jain, P. K., Lee, K. S., El-Sayed, I. H. & El-Sayed, M. A. Calculated absorption and scattering properties of gold nanoparticles of different size, shape, and composition: applications in biological imaging and biomedicine. *J. Phys. Chem. B* **110**, 7238–7248 (2006).
59. Bosbach, J., Hendrich, C., Stietz, F., Vartanyan, T. & Träger, F. Ultrafast dephasing of surface plasmon excitation in silver nanoparticles: influence of particle size, shape, and chemical surrounding. *Phys. Rev. Lett.* **89**, 257404 (2002).
60. Manjavacas, A., Liu, J. G., Kulkarni, V. & Nordlander, P. Plasmon-induced hot carriers in metallic nanoparticles. *ACS Nano* **8**, 7630–7638 (2014).
61. Atwater, H. A. & Polman, A. Plasmonics for improved photovoltaic devices. *Nat. Mater.* **9**, 205–213 (2010).
62. Brown, A. M., Sundararaman, R., Narang, P., Goddard, W. A. & Atwater, H. A. Nonradiative plasmon decay and hot carrier dynamics: effects of phonons, surfaces, and geometry. *ACS Nano* **10**, 957–966 (2016).
First-principles calculations of plasmon decay pathways in plasmonic nanostructures with analysis relating the decay pathways to the physical properties of the metals.
63. Bernardi, M., Mustafa, J., Neaton, J. B. & Louie, S. G. Theory and computation of hot carriers generated by surface plasmon polaritons in noble metals. *Nat. Commun.* **6**, 7044 (2015).
64. Sundararaman, R., Narang, P., Jermyn, A. S., Goddard Iii, W. A. & Atwater, H. A. Theoretical predictions for hot-carrier generation from surface plasmon decay. *Nat. Commun.* **5**, 5788 (2014).
65. Brongersma, M. L., Halas, N. J. & Nordlander, P. Plasmon-induced hot carrier science and technology. *Nat. Nanotech.* **10**, 25–34 (2015).
66. Knoesel, E., Hotzel, A. & Wolf, M. Ultrafast dynamics of hot electrons and holes in copper: excitation, energy relaxation, and transport effects. *Phys. Rev. B* **57**, 12812–12824 (1998).
67. Christopher, P., Xin, H., Marimuthu, A. & Linic, S. Singular characteristics and unique chemical bond activation mechanisms of photocatalytic reactions on plasmonic nanostructures. *Nat. Mater.* **11**, 1044–1050 (2012).
Combined experimental and theoretical study uncovering the role of hot carriers in plasmon-driven chemical reactions.
68. Mukherjee, S. et al. Hot-electron-induced dissociation of H_2 on gold nanoparticles supported on SiO_2. *J. Am. Chem. Soc.* **136**, 64–67 (2014).

69. Landry, M. J., Gellé, A., Meng, B. Y., Barrett, C. J. & Moores, A. Surface-plasmon-mediated hydrogenation of carbonyls catalyzed by silver nanocubes under visible light. *ACS Catal.* **7**, 6128–6133 (2017).
70. Zhu, H., Ke, X., Yang, X., Sarina, S. & Liu, H. Reduction of nitroaromatic compounds on supported gold nanoparticles by visible and ultraviolet light. *Angew. Chem.* **122**, 9851–9855 (2010).
71. Kim, Y., Wilson, A. J. & Jain, P. K. The nature of plasmonically assisted hot-electron transfer in a donor–bridge–acceptor complex. *ACS Catal.* **7**, 4360–4365 (2017).
72. Huang, Y.-F. et al. Activation of oxygen on gold and silver nanoparticles assisted by surface plasmon resonances. *Angew. Chem. Int. Ed.* **53**, 2353–2357 (2014).
73. Kim, Y., Dumett Torres, D. & Jain, P. K. Activation energies of plasmonic catalysts. *Nano Lett.* **16**, 3399–3407 (2016).
74. Upadhye, A. A. et al. Plasmon-enhanced reverse water gas shift reaction over oxide supported Au catalysts. *Catal. Sci. Technol.* **5**, 2590–2601 (2015).
75. Kazuma, E., Jung, J., Ueba, H., Trenary, M. & Kim, Y. Direct pathway to molecular photodissociation on metal surfaces using visible light. *J. Am. Chem. Soc.* **139**, 3115–3121 (2017).
76. Zhang, J. et al. Ag@Au concave cuboctahedra: a unique probe for monitoring Au-catalyzed reduction and oxidation reactions by surface-enhanced Raman spectroscopy. *ACS Nano* **10**, 2607–2616 (2016).
77. Xie, W. & Schlücker, S. Hot electron-induced reduction of small molecules on photorecycling metal surfaces. *Nat. Commun.* **6**, 7570 (2015).
78. Zhang, X. et al. Product selectivity in plasmonic photocatalysis for carbon dioxide hydrogenation. *Nat. Commun.* **8**, 14542 (2017).
79. Ageev, V. N. Desorption induced by electronic transitions. *Prog. Surf. Sci.* **47**, 55–203 (1994).
80. Misewich, J. A., Heinz, T. F. & Newns, D. M. Desorption induced by multiple electronic transitions. *Phys. Rev. Lett.* **68**, 3737–3740 (1992).
81. Shirhatti, P. R. et al. Observation of the adsorption and desorption of vibrationally excited molecules on a metal surface. *Nat. Chem.* **10**, 592–598 (2018).
82. Kale, M. J., Avanesian, T., Xin, H., Yan, J. & Christopher, P. Controlling catalytic selectivity on metal nanoparticles by direct photoexcitation of adsorbate–metal bonds. *Nano Lett.* **14**, 5405–5412 (2014).
83. Boerigter, C., Campana, R., Morabito, M. & Linic, S. Evidence and implications of direct charge excitation as the dominant mechanism in plasmon-mediated photocatalysis. *Nat. Commun.* **7**, 10545 (2016).
84. Palmer, R. E. & Rous, P. J. Resonances in electron scattering by molecules on surfaces. *Rev. Mod. Phys.* **64**, 383–440 (1992).
85. Yan, J., Jacobsen, K. W. & Thygesen, K. S. First-principles study of surface plasmons on Ag(111) and H/Ag(111). *Phys. Rev. B* **84**, 235430 (2011).
86. Boerigter, C., Aslam, U. & Linic, S. Mechanism of charge transfer from plasmonic nanostructures to chemically attached materials. *ACS Nano* **10**, 6108–6115 (2016).
Mechanistic study and analysis of energy transfer from plasmonic metals to molecules demonstrating the dominant role of the direct energy transfer mechanism.
87. Browne, W. R. & McGarvey, J. J. The Raman effect and its application to electronic spectroscopies in metal-centered species: techniques and investigations in ground and excited states. *Coord. Chem. Rev.* **251**, 454–473 (2007).
88. Wu, K., Chen, J., McBride, J. R. & Lian, T. Efficient hot-electron transfer by a plasmon-induced interfacial charge-transfer transition. *Science* **349**, 632–635 (2015).
89. Tan, S. et al. Plasmonic coupling at a metal/semiconductor interface. *Nat. Photon.* **11**, 806–812 (2017).
90. Kazuma, E., Jung, J., Ueba, H., Trenary, M. & Kim, Y. Real-space and real-time observation of a plasmon-induced chemical reaction of a single molecule. *Science* **360**, 521–526 (2018).
91. DuChene, J. S., Tagliabue, G., Welch, A. J., Cheng, W.-H. & Atwater, H. A. Hot hole collection and photoelectrochemical CO_2 reduction with plasmonic Au/p-GaN photocathodes. *Nano Lett.* **18**, 2545–2550 (2018).
92. Bauer, C., Abid, J.-P., Fermin, D. & Girault, H. H. Ultrafast chemical interface scattering as an additional decay channel for nascent nonthermal electrons in small metal nanoparticles. *J. Chem. Phys.* **120**, 9302–9315 (2004).
93. Hendrich, C. et al. Chemical interface damping of surface plasmon excitation in metal nanoparticles: a study by persistent spectral hole burning. *Appl. Phys. B* **76**, 869–875 (2003).
94. Foerster, B. et al. Chemical interface damping depends on electrons reaching the surface. *ACS Nano* **11**, 2886–2893 (2017).
95. Linnert, T., Mulvaney, P. & Henglein, A. Surface chemistry of colloidal silver: surface plasmon damping by chemisorbed iodide, hydrosulfide (SH^-), and phenylthiolate. *J. Phys. Chem.* **97**, 679–682 (1993).
96. Aslam, U., Chavez, S. & Linic, S. Controlling energy flow in multimetallic nanostructures for plasmonic catalysis. *Nat. Nanotech.* **12**, 1000–1005 (2017).
Systematic study illuminating the mechanism of energy transfer from plasmonic metals to catalytic metals.
97. Swearer, D. F. et al. Heterometallic antenna–reactor complexes for photocatalysis. *Proc. Natl Acad. Sci. USA* **113**, 8916–8920 (2016).
98. Zhang, C. et al. Al–Pd nanodisk heterodimers as antenna–reactor photocatalysts. *Nano Lett.* **16**, 6677–6682 (2016).
99. Mukherjee, J. & Linic, S. First-principles investigations of electrochemical oxidation of hydrogen at solid oxide fuel cell operating conditions. *J. Electrochem. Soc.* **154**, B919–B924 (2007).
100. Ingram, D. B. & Linic, S. First-principles analysis of the activity of transition and noble metals in the direct utilization of hydrocarbon fuels at solid oxide fuel cell operating conditions. *J. Electrochem. Soc.* **156**, B1457–B1465 (2009).

Acknowledgements

The work presented in this document was supported by the National Science Foundation (NSF) (CBET-1702471 and CHE- 1800197) (optical analysis) and Office of Basic Energy Science, Division of Chemical Sciences (FG-02-05ER15686) (materials synthesis). Secondary support for the development of analytical tools used to analyse the reaction kinetics was provided by the NSF (CBET-1436056). S.L. also acknowledges the partial support of the Technische Universität München – Institute for Advanced Study, funded by the German Excellence Initiative and the European Union Seventh Framework Programme under grant agreement no. 291763.

Competing interests

The authors declare no competing interests.

Additional information

Additional information

Reprints and permissions information is available at www.nature.com/reprints.

Correspondence should be addressed to S.L.

Publisher's note: Springer Nature remains neutral with regard to jurisdictional claims in published maps and institutional affiliations.